International Journal of Safety and Security Engineering
Vol. 16, No. 1, January, 2026, pp. 77-93
Journal homepage: http://iieta.org/journals/ijsse

Diagnosing Construction Deficiencies in Roller-Compacted Concrete Pavements on a University Campus Using Unmanned Aerial Vehicles

Jhon Paul Franco[1], Brayan Ronny Pinto[1,2], Eduardo Alberto Santos[1], Josué Briones-Bitar[1,2], Paúl Carrión-Mero[1,2], Fernando Morante-Carballo[2,3,4*]

[1] Facultad de Ingeniería en Ciencias de la Tierra (FICT), ESPOL Polytechnic University, ESPOL, Campus Gustavo Galindo, km. 30.5 Vía Perimetral, Guayaquil 090902, Ecuador
[2] Centro de Investigación y Proyectos Aplicados a la Ciencias de la tierra (CIPAT), ESPOL Polytechnic University, ESPOL, Campus Gustavo Galindo, km. 30.5 Vía Perimetral, Guayaquil 090902, Ecuador
[3] Facultad de Ciencias Naturales y Matemáticas (FCNM), ESPOL Polytechnic University, ESPOL, Campus Gustavo Galindo, km. 30.5 Vía Perimetral, Guayaquil 090902, Ecuador
[4] Geo-Recursos y Aplicaciones (GIGA), ESPOL Polytechnic University, ESPOL, Campus Gustavo Galindo, km. 30.5 Vía Perimetral, Guayaquil 090902, Ecuador

Corresponding Author Email: fmorante@espol.edu.ec

https://doi.org/10.18280/ijsse.160107

Received: 15 November 2025
Revised: 6 January 2026
Accepted: 21 January 2026
Available online: 31 January 2026

Keywords:
concrete pavement, Roller-Compacted Concrete Pavement, structural evaluation, structural rehabilitation, Unmanned Aerial Vehicle, sustainable infrastructure

ABSTRACT

Premature deterioration of concrete pavements remains a critical challenge to roadway performance, particularly when construction deficiencies and inadequate quality control reduce structural capacity and shorten service life. This study assessed the structural condition of a 1.5-km Roller-Compacted Concrete Pavement (RCCP) section at the entrance of a university campus and developed a technical rehabilitation plan in response to severe deterioration after only 12 years of service. The methodology comprised two phases: (i) inspection and analysis through field surveys, Unmanned Aerial Vehicle (UAV)-based mapping, and semi-destructive (SD) and non-destructive (ND) tests, including rebound hammer, core extraction, carbonation depth, and Ultrasonic Pulse Velocity (UPV); and (ii) diagnosis and rehabilitation planning based on technical standards and pavement engineering guidelines. The results identified multiple construction deficiencies, including irregular slab dimensions, thickness variability from 19 to 26 cm, internal voids, and longitudinal joints with widths ranging from 1 to 3 cm. Field surveys showed that 21.83% of the slabs exhibited distress, whereas the UAV survey captured up to 95% of the visible distress in the test segment, indicating strong potential for preliminary rigid pavement assessment. Mechanical testing further confirmed inadequate concrete quality, with compressive strength values as low as 8.14 MPa. Recommended rehabilitation measures included partial-slab (full-depth) or full-slab replacement, joint sealing, and crack treatment using low-modulus silicone sealant or epoxy resin. This study provides a replicable diagnostic framework integrating field inspection, SD and ND testing, and UAV technologies for the evaluation and rehabilitation of rigid pavements affected by construction deficiencies.

1. INTRODUCTION

Road infrastructure is a critical component of the socioeconomic development of nations, facilitating territorial connectivity, the mobility of goods and people, and access to essential services [1]. Since ancient times, roads have been constructed to promote trade and cultural expansion, evolving from simple dirt paths to complex paved structures [2]. Today, roadway development represents one of the sectors with the highest investment in infrastructure, with more than 900 billion dollars allocated annually worldwide for the construction and rehabilitation of roadways, according to World Bank data. However, the proper maintenance of these infrastructures remains a global challenge, particularly in developing countries [3].

From a technical perspective, pavements are classified as flexible, rigid, or composite. Rigid pavements, formed by concrete slabs, generally offer longer service lives, with design cycles that can exceed 30 years under adequate conditions [4]. Despite their durability, rigid pavements are susceptible to deterioration due to traffic loads and environmental factors [5]. Recent studies indicate that annual expenditures on road maintenance and rehabilitation amount to between 1.5% and 2.5% of GDP in many Latin American countries, highlighting the importance of optimising roadway asset management processes [6].

Within construction techniques, Roller-Compacted Concrete Pavement (RCCP) has proven to be an effective solution for rigid pavement construction due to its low water content, high compaction, and reliable mechanical

performance [7]. However, construction errors combined with natural material aging and traffic-induced erosion can accelerate deterioration and reduce service life, leading to distress such as cracking, potholes, surface erosion, and joint deterioration, as documented in national and international projects [8]. The rehabilitation of a rigid pavement requires a multidisciplinary analysis that considers structural evaluation, functional diagnosis, and economic and environmental assessment [9]. Various authors emphasise the need for methodologies that integrate visual inspections, destructive, semi-destructive (SD), and non-destructive (ND) tests, and georeferenced tools to determine the actual condition of pavement infrastructure. Furthermore, intervention strategies must adapt to local traffic conditions, climate, and resource availability to ensure more sustainable solutions [10].

Current trends in RCCP rehabilitation include technologies such as UV-resistant hybrid polyurethane–silicone sealants (Germany, Canada); ultra-high-performance concrete (UHPC) for deep repairs with service lives exceeding 50 years (France, Switzerland, Germany) [11]; diamond grinding to restore macrotexture and reduce the International Roughness Index (IRI) [12]; smart monitoring systems with embedded sensors to measure moisture and strains in real time (Australia, South Korea) [13]; and in-situ recycling of demolished slabs as stabilized subbase (Netherlands, Sweden), which can reduce carbon footprint by more than 30%. Nevertheless, many of these modern procedures face challenges to adoption in Latin American countries, which still struggle to develop and maintain roadway infrastructure [14].

Although several studies have investigated the performance and rehabilitation of Roller-Compacted Concrete (RCC) pavements, most existing methodologies have been developed and validated under temperate climatic conditions and in contexts with strict construction quality control. For example, Chhorn et al. [15] analyse the mechanical behaviour and compaction control of RCCP in East Asian projects, highlighting the influence of site parameters on structural performance.

Similarly, the behaviour of RCCP under hot climatic conditions has been evaluated, demonstrating that ambient temperature and curing methods influence mechanical and physical properties [16]. In terms of structural evaluation methodologies, ND techniques such as Ultrasonic Pulse Velocity (UPV) are used to estimate the quality of RCCP [17].

Consequently, its direct applicability in tropical environments and developing countries remains limited. In Latin America, rigid pavements are frequently exposed to high rainfall, high temperatures, accelerated material ageing, and poor construction practices, factors that significantly influence their structural behaviour and deterioration mechanisms. However, there is a notable lack of integrated assessment frameworks specifically adapted to these conditions.

In Ecuador, university roadway infrastructure also faces challenges related to material ageing, construction deficiencies, and inadequate maintenance. The Gustavo Galindo campus of the Escuela Superior Politécnica del Litoral (ESPOL), located in Guayaquil, has an internal network of rigid pavements that connect its main entrances and academic areas. These roads, initially designed for moderate traffic, currently support daily flows of more than 14,000 students, faculty, administrative staff, service personnel, and visitors. One of the most heavily used access routes to ESPOL is the roadway segment extending from the main entrance to the Prosperina interchange, with an approximate length of 1.5 km and a width of 22 meters (Figure 1). This roadway consists of two dual-lane carriageways and a central median. Its construction with RCCP was completed in 2012 to alleviate vehicular congestion at the campus entrance, which at the time relied on a single access point. Currently, early and accelerated deterioration of the concrete pavement slabs has become evident, with distress such as longitudinal and transverse cracking, aggregate loss, loss of slab smoothness, and joint deterioration. The absence of an integral intervention not only affects roadway safety but also increases vehicle operating costs and negatively impacts academic and operational productivity on campus [10].

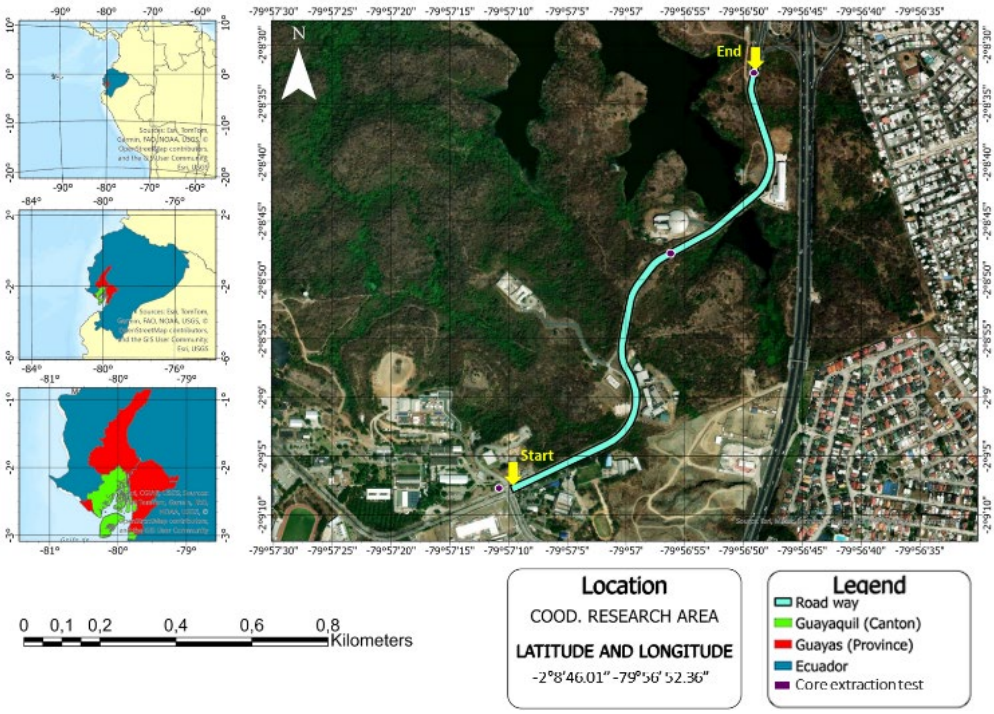

Figure 1. Location of the Roller-Compacted Concrete Pavement (RCCP) pavement section evaluated

In response to this problem, the following question arises: Which preventive and corrective maintenance measures enable the structural rehabilitation of this roadway segment? Accordingly, this study evaluated the structural condition of the pavement slabs through in-situ inspections and a combination of SD and ND tests, complemented by a pilot Unmanned Aerial Vehicle (UAV)–based survey, to develop a structural rehabilitation proposal for the rigid pavement section based on technical standards and pavement engineering guidelines, aligned with Sustainable Development Goals (SDGs) 9 and 11. Additionally, the use of UAV technology was validated as a diagnostic tool for assessing roadway conditions.

2. METHODOLOGY

This section describes the materials and procedures used to evaluate the structural condition of the concrete pavement slab. The methodological process combined field inspections, laboratory tests and technical standards to diagnose the main types of distress and define rehabilitation strategies that optimise the safety, functionality, and durability of the studied roadway. The methodological framework applied in this study is presented in Figure 2 and consists of two phases.

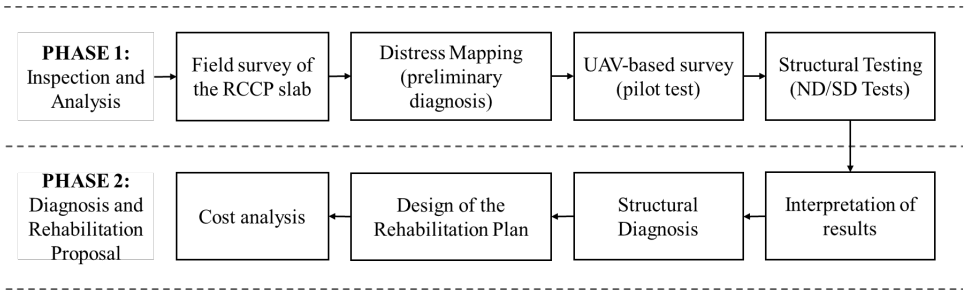

Figure 2. Methodological framework for pavement slab evaluation and rehabilitation proposal
Note: non-destructive (ND); semi-destructive (SD); Roller-Compacted Concrete Pavement (RCCP).

2.1 Phase 1: Inspection and analysis

A damage survey of the pavement slab was conducted through field inspections performed by specialized technical personnel [18], identifying distress such as potholes, cracks, surface erosion, joint sealant deficiencies, and slab smoothness, heave, and settlement. For the identification and grouping of damages, the *Manual for the visual inspection of rigid pavements* [19] was used as the technical reference. A pilot UAV flight was then performed over a segment of the roadway to acquire aerial imagery of the pavement and compare the damage captured from the drone with that recorded during the in-situ survey [20]. Subsequently, several tests were performed to characterize the structural condition of the pavement [20].

2.1.1 Field survey of the Roller-Compacted Concrete Pavement slab and distress mapping

The entire roadway was surveyed on-site, starting at the Start point shown in Figure 1 (station 0+000), covering all four lanes (two in each direction), and all observed distresses were recorded according to type and severity. To measure the dimensions of the distress, a tape measure, crack gauge, and measuring tape were used. At the same time, a camera and a GPS device were employed for photographic documentation and georeferencing. Table 1 summarizes the types of distress recorded, their groups, and the severity levels.

Table 1. Distress types, groups, and severity levels [19]

Type of Damage	Severity		
	Low	**Medium**	**High**
Surface distress		*d = depth; w = width*	
Pothole	d < 2.5 cm	2.5-5 cm	> 5 cm
Surface erosion	Surface paste loss	Generalized paste loss	Generalized loss of paste and coarse aggregate
Spalling	w < 5 cm	5-15 cm	> 15 cm
Slab heave and settlement		*dif = vertical differential*	
Localized slab settlement Localized slab heave	dif < 5 cm	5-10 cm	> 10 cm
Joint sealant deficiency		*l = % of joint length affected*	
Transverse joint sealant deficiency Longitudinal joint sealant deficiency	l < 5%	5-25%	> 25%
Cracking		*cw = crack width*	
Transverse crack Longitudinal crack Corner crack	cw < 3 mm	3-10 mm	> 10 mm

For surface distresses, the length (parallel to the roadway axis), width (perpendicular to the roadway axis), and depth were measured, except for erosion damage, where depth does not exceed 1.5 cm. For slab heave and settlement, the length, width, and vertical differential were measured. For joint sealant deficiencies and cracking, which are linear distresses, the total length of the deterioration was measured. In the case of cracks, their width was also recorded. Slab dimensions were recorded only when significant variations were observed. For joint sealant deficiency in transverse joints, the slab located

downstream of the joint in the direction of travel was considered the affected slab. For longitudinal joints, the slab on the right side in the direction of travel was taken as the affected slab. Slab numbering followed an alphanumeric convention, where each lane was assigned a letter and each row of slabs a number (Figure 3).

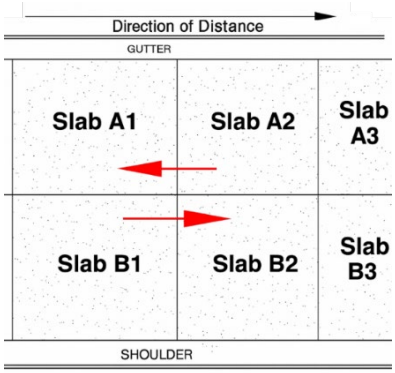

Figure 3. Slab numbering system [19]

For the analysis of the recorded distresses, the roadway was divided into ten segments, each 150 m long, except for the last segment, which is 203 m long. For the surface distress group, the affected area of each damage was computed using Eq. (1), as well as the total affected area. For the cracks and joint sealant deficiency groups, the total length was summed.

$$\text{Damage area} = \text{Length} \times \text{Width} \quad (1)$$

To identify the most affected sections of the roadway, for each segment, the total number of existing slabs and the number of damaged slabs were recorded. The sum of the total number of slabs in all segments corresponds to the total number of slabs along the roadway Eq. (2). Then, the percentage of affected slabs in each segment was calculated with respect to the total number of slabs in that segment Eq. (3) and with respect to the total number of slabs along the entire roadway Eq. (4).

That is, for each segment, the following were calculated, where i is the segment number:

$$\text{Total no. of slabs} = \sum_{1}^{10} \text{No. slabs in segment} \quad (2)$$

$$\%\ \text{of affected slabs in segment} = \frac{\text{No. of affected salbs}}{\text{No. slabs in segment}} \quad (3)$$

$$\%\ \text{of affected slabs globally} = \frac{\text{No. of affected salbs}}{\text{Total no. of slabs}} \quad (4)$$

This calculation was computed individually for each damage group and globally for all recorded damages combined.

2.1.2 Unmanned Aerial Vehicle–based survey (pilot test)

In addition to the in-situ distress survey, a pilot aerial survey was carried out using a DJI Mavic 2 Pro drone over the section of the roadway with the highest concentration of distress, between stations 1+309 and 1+359. Three flights were performed at altitudes of 60 m, 30 m, and 10 m, respectively, capturing aerial images of the pavement and documenting all visible slab damages. This test aimed to evaluate the potential of UAV-based aerial imagery as a complementary tool for pavement damage surveys, as suggested by recent studies [21].

Regarding UAV validation, a pilot aerial survey was conducted over a 50 m section, with the highest concentration of damage observed. This section was intentionally selected to maximize the probability of detecting damage patterns and to assess the feasibility of UAV imagery as a complementary diagnostic tool. Given the limited length studied, the UAV results are presented as preliminary and should not be extrapolated to the entire 1.5 km of the road.

2.1.3 Structural testing

After documenting all distresses, critical areas, and representative damages, the SD tests (concrete core extraction and compressive testing) and ND tests (rebound hammer, carbonation depth, and UPV) were conducted to characterise the structural condition of the rigid pavement slab.

First, concrete cores were extracted and tested in compression to determine the actual concrete strength. Then, rebound hammer testing was performed to estimate surface hardness, complementing the core extraction results. Additionally, carbonation depth was evaluated on the extracted concrete cores, and finally, UPV testing was carried out to assess crack depth and complement the structural diagnosis. Historical information was also collected, including technical reports, civil engineering theses, and applicable standards such as ACI 546R-14 [22], ASTM C42 [23], ASTM C597 [24], ASTM C805 [25], and UNE-EN 14630:2007 [26]. The tests performed are described below.

Concrete Core Extraction and compressive testing. This SD test provides a highly reliable measurement of the compressive strength of the pavement concrete by extracting cylindrical concrete cores and testing them in a hydraulic press [27]. The test was performed in accordance with ASTM C42 [23] using 100-mm-diameter cores and applying strength correction factors based on the length-to-diameter ratio (Table 2).

Table 2. Strength correction factors [20]

Length-to-Diameter Ratio (L/D)	Strength Correction Factor
1.75	0.98
1.50	0.96
1.25	0.93
1.00	0.87

Core extractions were performed at stations 0+24 and 1+460, and an additional core was extracted from a pavement slab inside the ESPOL campus, located 69 m from the beginning of the roadway (Figure 1). The coring system used was a Milwaukee Dymodrill with a Husqvarna Vari-Drill D65 57 × 500 1 1/4" bit (Figure 4).

Concrete cores were extracted every 750 m, selecting three representative locations along the road section. The drilling points were determined based on prior visual inspection, prioritising areas with severe damage, such as extensive cracking, advanced surface deterioration, and cavities. Although the number of cores extracted limits the statistical robustness of the compressive strength estimate, the results obtained provide indicative and exploratory information on the structural condition of the most affected areas of the pavement. Consequently, these values should be interpreted as a diagnostic approximation rather than as a comprehensive statistical characterisation of the entire section studied.

Rebound hammer test. This ND test is widely used due to its simplicity and low cost. It evaluates the concrete's surface hardness and identifies areas of lower quality by relating surface hardness to the rebound index (R). The test was performed in accordance with ASTM C805 [25]. Data processing followed the guidelines of the manufacturer of the Kamekura Seiki Concrete Test Hammer R-7500 [28] (Figure 5).

Figure 4. Core extraction equipment (Milwaukee Dymodrill)

Figure 5. Rebound hammer (Kamekura Seiki Concrete Test Hammer R-7500)

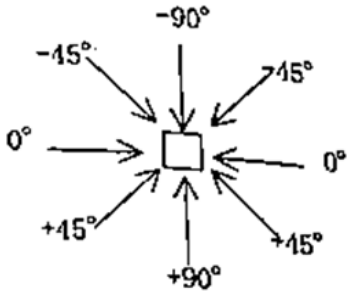

Figure 6. Rebound hammer reading angle [25]

Test locations for the rebound hammer test were selected at regular intervals of 150 m along the study section. The measurement points were defined based on a preliminary visual inspection, prioritising slabs exhibiting evidence of deterioration, such as cracks, surface wear, material loss, and other pathologies affecting the pavement's structural performance.

The orientation of impact reading (Figure 6) was selected as −90°. A direction correction factor ΔR (Table 3) of +3, a moisture correction factor ΔRw (Table 4) of +0, and an age factor α_n (Table 5) of 0.63 (corresponding to the 12-year-old structure) were applied.

Table 3. Impact direction correction factor ΔR [28]

R	ΔR			
	+90	+45	-45	-90
20	-6	-4	+2	+3
30	-5	-3	+2	+3
40	-4	-3	+2	+2
50	-3	-2	+1	+2
60	-2	-2	+1	+2

Table 4. Moisture correction factor ΔRw [28]

Apparent Moisture Condition	ΔRw
Surface is dry	+0
Surface is damp	+3
Surface is wet	+5

Table 5. Age factor α_n [28]

Age n (days)	α_n
10	1.55
20	1.12
28	1.00
50	0.87
100	0.78
150	0.74
200	0.72
300	0.70
500	0.67
1000	0.65
3000	0.63

After obtaining the rebound index R, a corrected index Rc was computed using Eq. (5). The concrete surface strength at each evaluated point was then calculated using Eq. (6). This test was conducted approximately every 200 m along the pavement slab.

$$Rc = R + \Delta R + \Delta Rw \quad (5)$$

$$f'c\ (MPa) = 0.098\ (-184+13\ Rc) \times \alpha_n \quad (6)$$

Carbonation depth test. This ND test determines the depth of the carbonated layer in the concrete using a 1% phenolphthalein solution in a hydroalcoholic medium (70% alcohol and 30% water), in accordance with UNE-EN 14630:2007 [26]. When applied (Figure 7), carbonated concrete does not turn magenta, whereas sound concrete with a pH > 12 does. This test was performed on all extracted concrete cores.

Figure 7. Phenolphthalein solution used for carbonation testing

UPV test. The ultrasonic test in concrete is useful for identifying cracks and measuring their depth of influence [29], as shown in Figure 8.

Figure 8. Pulse generator (Toyoko Elmes)

The test was carried out in accordance with ASTM C597 on representative cracks in the slab at stations 0+254, 1+163, 1+229, 1+335, and 1+452. To calculate crack depth (Figure 9), the equipment uses the following parameters and calculations, Eq. (7), based on the BS 1881 Part 203 method [30]:

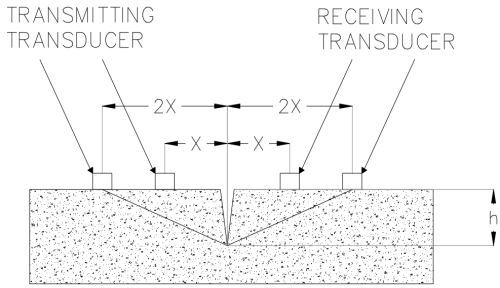

Figure 9. Crack depth measurement through Ultrasonic Pulse Velocity (UPV) test

Being:

X: initial distance between the crack and each transducer.

t_1: wave travel time with the transducers located at a distance X from the crack.

t_2: wave travel time with the transducers located at a distance 2X from the crack.

h: crack depth.

$$h = X*\left(\frac{4t_1^2 - 4t_2^2}{4t_2^2 - 4t_1^2}\right)^{0.5} \quad (7)$$

2.2 Phase 2: Diagnosis and rehabilitation proposal

In this phase, the results from laboratory tests were first analysed to develop a structural assessment of the rigid pavement slab. This information was used to support the technical proposals for its rehabilitation and the cost analysis. For the selection and technical description of the rehabilitation procedures, the *Manual for the design and construction of concrete pavements* by the Argentine Portland Cement Institute, authored by Calo et al. [31], and *Guide for concrete pavement distress assessments and solutions: Identification, causes, prevention, and repair* by Harrington et al. [32] were used as technical references. Among the proposed rehabilitation solutions for the concrete pavement slab, partial-slab (full-depth) or full-slab replacement was included, along with joint sealing and crack treatment using low-modulus silicone sealant or epoxy resin. These measures aim to restore the structural capacity of the pavement within the university campus.

3. RESULTS AND DISCUSSION

3.1 Distresses survey and mechanical performance of concrete

3.1.1 Evidence of construction deficiencies

Field inspection revealed multiple indications of deficiencies in the construction process of the evaluated concrete pavement slab. Significant variations were identified in slab dimensions, with widths ranging from 3.20 to 3.50 m and lengths from 4.10 to 4.85 m (Table 6). These slab dimensions differ from the 3.40 m width and 4.40 m length of the design, suggesting insufficient control during joint cutting. It is worth mentioning that joint spacing is a fundamental parameter in the design and construction of concrete pavements, as it governs slab dimensions and therefore the stresses generated by curling and warping [33]. Therefore, these geometric irregularities compromise stress distribution and may promote the development of premature cracking.

Table 6. Slab dimensions

Station	Outbound Carriageway			Inbound Carriageway		
	Width (m)		Length (m)	Width (m)		Length (m)
	Left Lane	Right Lane		Left Lane	Right Lane	
0+000	3.60	3.50	4.70	3.40	3.38	4.20
0+200	3.40	3.40	4.29	3.40	3.40	4.31
0+400	3.40	3.37	4.65	3.40	3.40	4.51
0+600	3.40	3.37	4.40	3.20	3.23	4.40
0+800	3.33	3.30	4.18	3.20	3.21	4.85
1+000	3.30	3.46	4.10	3.36	3.40	4.23
1+200	3.40	3.40	4.53	3.38	3.41	4.40
1+400	3.40	3.40	4.50	3.40	3.40	4.56
1+488	3.40	3.40	4.35	3.40	3.40	4.35

Similarly, an irregular gap was detected between the slab and the curb along the longitudinal joint, ranging from 1 to 3 cm across the roadway (Table 7), in contrast to the typical 3-6 mm design range [31]. This abnormal separation indicates that the pavement was likely cast after the curb, leaving a void prone to the intrusion of water and incompressible materials. Such a condition promotes the expulsion of water and fines under traffic loading, generating loss of support and slab cracking due to the pumping mechanism [32]. This condition is considered another distress group among the solutions proposed in the following sections.

Table 7. Width of the longitudinal joint between the slab and the curb

Station	Longitudinal Joint Width Between Slab and Curb (cm)	
	Inbound Roadway	Outbound Roadway
0+000	1.5	1.5
0+200	0.7	1
0+400	1	3
0+600	3	1
0+800	2	3
1+000	3	2
1+200	2	2
1+400	2	2
1+488	1	3

Field observations also revealed widespread cracking across the pavement slabs, including longitudinal, transverse, and corner cracks in all roadway segments. A critical case was observed at station 1+377, where three adjacent slabs exhibited full-depth cracking (Figure 10(a)). This crack developed next to a longitudinal slab-to-curb joint with an irregular 3 cm width (Figure 10(b)). The widespread cracking is attributed to a combination of factors, including deficiencies during RCCP compaction—affecting final strength—and the loss of slab support caused by pumping, aggravated by the oversized longitudinal joint, as further discussed in the following section.

The presence of severe full-depth cracking and the oversized longitudinal joint also enabled direct measurements of the slab thickness (Figure 10(c)). Thicknesses ranged from 19 to 23 cm, with an average of 21.81 cm (Table 8), evidencing inconsistent construction practices and deficient quality control. It is worth noting that the measured thickness exceeds the recommended limit for aggregate-interlock jointed concrete pavements (18 cm) [31], suggesting possible shortcomings in the original structural design.

Overall, these observations reflect construction errors and deficiencies in quality control that reduce the structural integrity of the concrete pavement and partially explain the premature surface and full-depth distresses documented through laboratory testing.

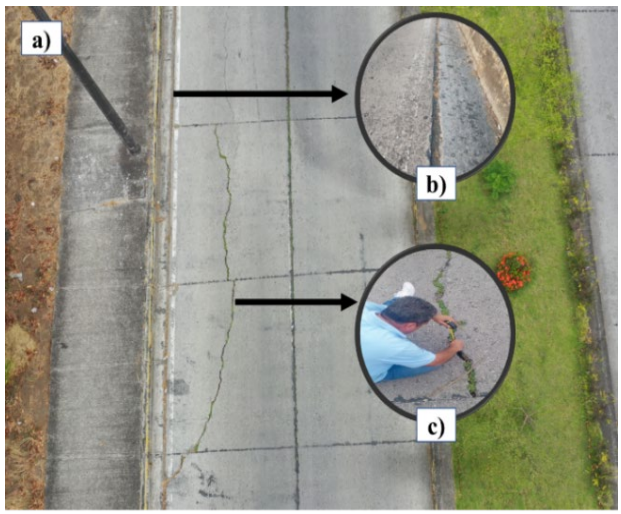

Figure 10. Construction deficiencies and full-depth cracking (station 1+340)

Table 8. Measured slab thickness values

Station	Thickness (cm)	Observation
0+858	23	Gap of 3 cm between the slab and the curb
0+861	22	
0+864	23	
0+869	21	
0+874	22	
0+884	23	
0+886	23	
0+890	23	
1+340	22	Full-depth longitudinal crack affecting three slabs, maximum width 3 cm
1+342	23	
1+343	22	
1+345	21	
1+345	21	
1+349	20	
1+351	21	
1+352	19	
Average	21.81	

Table 9. Distress survey using Unmanned Aerial Vehicle (UAV) in a road segment (stations 1+309 to 1+359)

Type of Distress	No. Distresses Recorded			
	In-Situ Survey	UAV Survey		
		60 m	30 m	10 m
Pothole	10	0	8	10
Surface erosion	10	0	10	10
Transverse hairline crack	6	0	3	4
Longitudinal hairline crack	2	0	2	2
Longitudinal crack	2	0	2	2
Corner crack	3	0	2	3
Longitudinal joint sealant deficiency	5	0	3	5
Transverse joint sealant deficiency	2	0	1	2
Percentage	100%	0%	78%	95%

3.1.2 Unmanned Aerial Vehicle–based distress survey validation

Aerial photographs of the pavement slabs between stations 1+309 and 1+359 were reviewed to document distress, and the results are presented in Table 9.

Using the drone model selected for the test, the flight at 60 m height did not allow identification of slab distress (Figure 11(a)). At 30 m, 78% of the distresses recorded during in-situ inspection were detected (Figure 11(b)). At 10 m, this percentage increased to 95% (Figure 11(c)). These results support recent literature highlighting the potential of drones as an affordable tool for pavement distress surveys over large areas in short time periods [21], with accuracy further enhanced by implementing photogrammetry and machine learning algorithms [34]. The recommended flight height will depend on drone model and data processing method; however, the identified optimal height of 10 m is consistent with studies recommending low-altitude flights, typically 5–10 m, to maximize image-based distress detection accuracy [35].

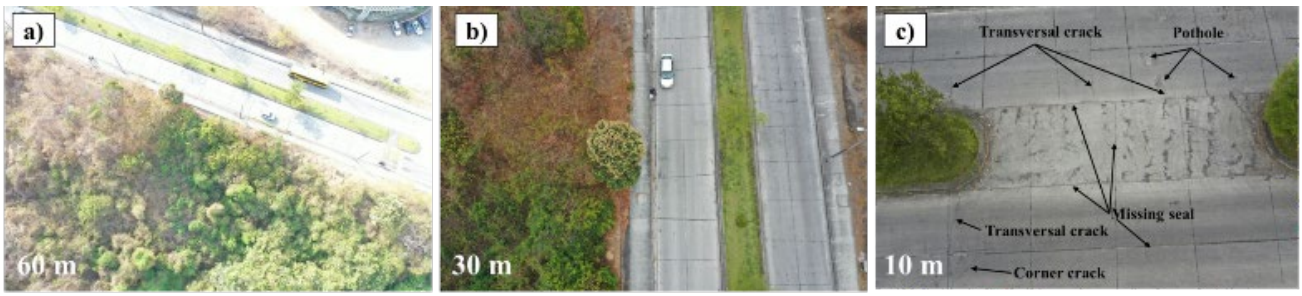

Figure 11. Distress photographs captured with Unmanned Aerial Vehicle (UAV) at different altitudes (stations 1+309 to 1+359)

3.1.3 Core extraction, rebound hammer testing, and carbonation depth

The analysis of concrete strength and quality through SD and ND testing revealed marked variability in the mechanical performance of the slabs, primarily attributable to construction deficiencies. Core extractions provided the most reliable reference, yielding compressive strengths of 19.07 MPa at station 0+724 and only 8.14 MPa at station 1+460 (Table 10). Pronounced internal voids were clearly visible in the core extracted at the latter location (Figure 12).

Table 10. Compressive strength obtained from core extractions

Station	Extracted Length (mm)	Tested Length (mm)	Diameter (mm)	Compressive Strength (MPa)
0+724	260	200	100	19.07
1+460	230	200	100	8.14
Campus interior slab	135	130	100	27.79

Figure 12. Voids in concrete core (station 1+460)

These strength values fall well below what is expected for concrete pavements carrying heavy traffic (~30 MPa) [33], confirming the low structural performance of the concrete. In addition, the extracted cores showed a maximum slab thickness of 26 cm (Table 10), greater than the previously measured 23 cm (Table 9), indicating even greater variability in slab thickness.

In contrast, the core extracted from the pavement slab inside ESPOL, constructed only one year earlier, showed a thickness of 13.5 cm and a compressive strength of 27.79 MPa (Table 11), within the expected range for properly compacted RCCP. This difference reinforces the hypothesis of irregular construction processes in the study pavement. The presence of internal voids observed in multiple specimens confirms problems with concrete compaction during slab construction.

The rebound hammer test showed an average surface strength of 18.41 MPa (Table 11), consistent with the trends observed in the cores but with greater variability among locations. The comparison between the two methods indicated that rebound hammer testing is useful as a preliminary exploratory tool but insufficient as a standalone evaluation method due to factors such as hammer impact on coarse aggregates, carbonation effects, and inherent limitations of manufacturer correlations [36]. Nonetheless, acceptable correspondence at specific locations supports the complementary use of both tests.

The carbonation test performed on the extracted cores showed a uniform penetration of 3 mm (Table 12), indicating minimal surface carbonation. Since the pavement uses aggregate-interlock joints without dowels, carbonation is not a governing factor in the observed deterioration and does not explain the recorded loss of structural capacity.

The compressive strength values shown in Table 10, obtained from core extraction (8.14 MPa and 19.07 MPa), are based on a limited number of test points, which limits statistical treatment. Consequently, these results are presented as indicative and exploratory, and not as a comprehensive statistical characterization of the entire pavement section.

However, the marked contrast between the measured values

indicates variability in concrete quality along the road. The more than 10 MPa difference between cores extracted from different segments indicates heterogeneity attributable to variability in compaction and construction control, resulting in internal voids, surface deterioration, and thickness variability observed during the field inspection.

Regarding the relationship between mechanical performance and damage frequency, this study does not attempt to establish a statistical correlation due to the small sample size. Instead, a qualitative association was identified between areas with lower compressive strength, higher deterioration concentration, and greater construction deficiencies.

Table 11. Compressive strength obtained from the rebound hammer test

Station	f'c (MPa)
0+000	28.03
0+111	19.14
0+266	19.51
0+424	20.28
0+576	19.88
0+724	19.28
0+867	18.94
1+020	20.08
1+179	15.33
1+335	12.65
1+460	9.37
Average	18.41

Table 12. Carbonation depth in pavement slabs

Station	Extracted Length (mm)	Diameter (mm)	Carbonation Depth (mm)
0+724	200.0	100.00	3
1+460	200.0	100.00	3
Campus interior slab	130.0	100.00	3

3.2 Structural diagnosis and rehabilitation proposal

The overall percentage of affected slabs by segment is presented in Table 13. The results show that the most deteriorated areas are located in the final segments of the roadway, particularly between stations 1+200–1+350 and 1+350–1+488, where 31.08% and 45.52% of the slabs exhibit some distress, respectively. At the global level, more than one-fifth of the pavement slabs (21.83%) are affected. This deterioration pattern coincides spatially with the sections in which mechanical testing revealed the lowest compressive strength values, as well as with the locations where significant internal voids were identified in the concrete cores. This suggests a strong correlation between the constructive quality of the pavement and the frequency and severity of the observed distresses.

The analysis of slab distress allowed classification into four main distress groups: surface distress, joint sealant deficiency, cracking, and slab heave/settlement. Each group reflects distinct degradation mechanisms but remains linked to the construction deficiencies and low mechanical performance previously identified. To categorize deep distresses, damages affecting more than the upper one-third of the slab thickness (depth > 7 cm) were considered [32]. The following subsections present detailed results for each distress group, integrating both field observations and laboratory test results.

Table 13. Overall distress affecting slabs by segments

N°	Initial Station	Final Station	No. Affected Slabs	No. of Slabs in the Segment	% Affected Slabs within the Segment	% Affected Slabs Relative to All Slabs
1	0+000	0+150	26	156	16.67%	1.79%
2	0+150	0+300	23	140	16.43%	1.58%
3	0+300	0+450	39	140	27.86%	2.69%
4	0+450	0+600	15	148	10.14%	1.03%
5	0+600	0+750	26	136	19.12%	1.79%
6	0+750	0+900	26	136	19.12%	1.79%
7	0+900	1+050	22	154	14.29%	1.52%
8	1+050	1+200	33	160	20.63%	2.27%
9	1+200	1+350	46	148	31.08%	3.17%
10	1+350	1+448	61	134	45.52%	4.20%
Total			**317**	**1452**		**21.83%**

3.2.1 Surface distress

Surface distress was the most frequent damage group in the pavement, affecting approximately 11.85% of the evaluated slabs (Table 14). This group includes potholes, surface erosion, and spalling, which were primarily observed in the final segments of the roadway. During the visual inspection, surface erosion was observed, characterised by the progressive loss of paste and coarse aggregate over extensive slab areas, predominantly at high severity (Figure 13(a)). This pattern is consistent with poorly compacted concrete and the presence of internal voids observed in the extracted cores—conditions that reduce slab durability and accelerate abrasion-related disintegration, being compaction, a well-known key factor influencing RCCP performance [37].

Potholes with depths of up to 10 cm were recorded, representing a high severity level (Figure 13(b)) and directly compromising the structural capacity of the slab due to their classification as serious damage. Potholes of this magnitude pose a significant safety hazard to users, potentially leading to traffic accidents, operational disruptions, and vehicle damage. Spalling appeared less frequently but was concentrated in the segments with the highest overall deterioration toward the end of the roadway. This type of damage typically occurs when joints lack adequate sealing, allowing the intrusion of incompressible material, which, under repeated loading, induces fracture stresses at the slab edges (Figure 13(c)) [38].

Table 14. Distress by segments: Surface distress

N°	Initial Station	Final Station	% Affected Slabs Relative to All Slabs	No. Affected Slabs by Severity Level (L: Low; M: Medium; H: High)		
				L	M	H
1	0+000	0+150	1.31%	2	9	9
2	0+150	0+300	0.41%	2	3	2
3	0+300	0+450	1.72%	1	12	13
4	0+450	0+600	0.76%	6	4	3
5	0+600	0+750	0.83%	4	9	2
6	0+750	0+900	0.76%	1	8	3
7	0+900	1+050	0.69%	2	4	4
8	1+050	1+200	1.10%	4	10	4
9	1+200	1+350	1.93%	3	15	12
10	1+350	1+553	2.34%	8	22	8
Total			**11.85%**	**33**	**96**	**60**

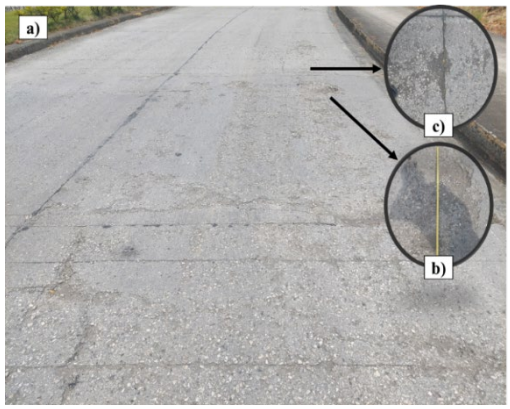

Figure 13. Surface distress on pavement slab (station 0+558)

Figure 14. Slab joints and distress reflected on the asphalt overlay (station 1+040)

This condition aligns with field observations indicating the absence or severe deterioration of joint sealant material in several joints, promoting the progressive formation of spalling at slab edges. Moreover, it was found that in a roadway segment near the ESPOL lake (station 1+040), an asphalt overlay had been placed over the rigid pavement slab, which already reflects on its surface the joints, potholes, cracks, and wide cracks of the underlying slab (Figure 14).

Overall, the surface distress group reflects an accelerated deterioration process attributable to the low final concrete strength resulting from poor compaction and to pumping mechanisms triggered by inadequately sealed joints. This pattern coincides with the critical strength values obtained from core extractions in the final roadway segments, where the largest affected areas were recorded.

3.2.2 Joint sealant deficiency

The deficiency of joint sealant in longitudinal and transverse joints affected 4.82% of the evaluated slabs, with severe levels of deterioration concentrated in the final segment of the roadway (Table 15). In numerous areas, the longitudinal joints exhibited complete absence, severe deterioration, or discontinuity of the sealant, allowing vegetation growth and the intrusion of water and incompressible materials.

Table 15. Distress by segments: Joint sealant deficiency

N°	Initial Station	Final Station	% Affected Slabs Relative to All Slabs	No. Affected Slabs by Severity Level (L: Low; M: Medium; H: High)		
				L	M	H
1	0+000	0+150	0.14%	0	0	2
2	0+150	0+300	0.69%	0	0	10
3	0+300	0+450	0.00%	0	0	0
4	0+450	0+600	0.21%	0	0	3
5	0+600	0+750	0.34%	0	0	5
6	0+750	0+900	0.83%	0	0	12
7	0+900	1+050	0.62%	0	0	9
8	1+050	1+200	0.14%	0	0	2
9	1+200	1+350	0.14%	0	0	2
10	1+350	1+553	1.72%	0	0	25
Total			**4.82%**	**0**	**0**	**70**

Progressive infiltration generated pumping under repeated traffic loads and accelerated loss of support at slab edges, contributing to the development of spalling associated with the pressure exerted by trapped incompressible materials (Figure 15(a)). In the transverse joints, a poorly executed maintenance process was observed, with sealant material accumulating on the slab surface and application performed without adequate surface preparation (Figure 15(b)). Such deficiencies

compromise the adhesion of the sealant and accelerate its loss due to traffic abrasion [39].

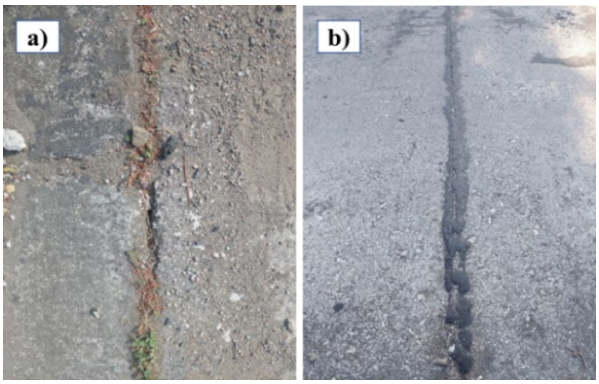

Figure 15. Joint sealant deterioration: (a) Station 1+414; (b) Station 0+085

The condition of the joints was further aggravated by the presence of irregular widths between the slab and the curb, ranging from 1 to 3 cm along the roadway—values inconsistent with concrete pavement joint design criteria, which typically range from 3–6 mm. These irregular openings not only facilitated water infiltration but also made it difficult to seal the longitudinal joint using fluid-applied sealants.

Overall, the evidence indicates that joint sealant deficiency, stemming from both construction defects and the absence (or improper execution) of joint maintenance, constitutes a major mechanism of pavement degradation. The combined effects of incompressible material intrusion and progressive support loss due to pumping created favourable conditions for the development of spalling and cracking, which are analysed in the following section.

3.2.3 Cracking

Cracking constitutes one of the most relevant damage groups in the pavement, affecting 8.82% of the evaluated slabs, particularly those located in the final segments of the roadway (Table 16).

The results of the UPV test showed the presence of both shallow and deep cracks (Table 17), such as the transverse crack at station 1+453, evaluated immediately before a slab exhibiting a full-depth crack. The evidence presented in previous sections suggests that inadequate or poorly executed maintenance of the joint sealant—combined with the low concrete strength—is the main factor contributing to the presence and progression of cracks in the pavement slabs.

Table 16. Distress by segments: Cracking

N°	Initial Station	Final Station	% Affected Slabs Relative to All Slabs	No. Affected Slabs by Severity Level (L: Low; M: Medium; H: High)		
				L	M	H
1	0+000	0+150	0.76%	11	0	0
2	0+150	0+300	0.62%	9	0	0
3	0+300	0+450	1.17%	14	4	1
4	0+450	0+600	0.28%	4	0	0
5	0+600	0+750	0.96%	14	0	0
6	0+750	0+900	0.48%	1	0	6
7	0+900	1+050	0.41%	4	2	0
8	1+050	1+200	1.31%	14	2	4
9	1+200	1+350	1.38%	5	12	4
10	1+350	1+553	1.45%	10	11	1
	Total		**8.82%**	**86**	**31**	**16**

Table 17. Depth of cracks in pavement slab – Ultrasonic Pulse Velocity (UPV) test

Station	Type of Crack	Length (cm)	Width (cm)	Depth (cm)
0+254	Transverse crack	340	0.2	6.15
1+164	Transverse crack	340	0.2	1.80
1+229	Corner crack	172	0.4	4.15
1+335	Longitudinal crack	440	0.2	8.60
1+453	Transverse crack	340	0.2	4.06

3.2.4 Slab heave and settlement

Slab heaves and settlement constitute a less frequent distress group compared with others, yet they have a significant impact on pavement serviceability, as they generate considerable discomfort for roadway users. This distress affected approximately 0.55% of the evaluated slabs, with only eight localized settlements identified. Slab settlement is closely associated with the pumping mechanism, and during the field survey, it was found adjacent to joints lacking proper sealant. Moreover, the presence of longitudinal joints with abnormal widths between the slab and the curb also contributed to slab settlement by allowing water infiltration.

3.2.5 Proposed rehabilitation procedures and costs

Overall, the diagnosis identifies three predominant deterioration mechanisms that explain the distribution and severity of the pavement distress. First, the low concrete strength and the presence of internal voids, evidenced in the extracted cores, promoted surface distress, accelerated surface erosion, and the formation of potholes, particularly in the final segments of the roadway. Second, the Deficiency of Joint Sealant—along with poorly executed maintenance of the sealant—allowed the intrusion of water and incompressible material, resulting in progressive loss of support due to pumping, and the development of spalling and cracking. Finally, the presence of abnormally wide longitudinal joints facilitated water infiltration, contributing to localized slab settlement and the formation of associated cracks. Based on the diagnostic findings from the pavement slab evaluation, the proposed technical strategy prioritises selective, staged interventions, following the principles established in the *Concrete Pavement Preservation Guide* [38].

For the surface distress group, the recommended solution is the partial-slab (full-depth) replacement or full-slab replacement, using hydraulic concrete with a compressive strength of 30 MPa, depending on the area and severity of the identified damage. The repair area must span the full width of the slab and have a minimum length of 220 cm (approximately half a slab) [31]. The repair work must include joint sealing, and, when loss of slab support is detected, reconstruction of the support layer using a Type 2 subbase. Partial-depth repairs are not recommended due to the thermal incompatibility between the existing RCCP slab and repair concrete [31], and because most slabs exhibit multiple deep and widespread distress. A seemingly simple solution, such as placing an asphalt overlay, would only provide temporary benefits and would not prevent reflective cracking or distress propagation from the underlying slab, as noted by Treviño et al. [40] and Riekstins et al. [41]. This condition is evident in the asphalt overlay applied over the pavement slab near the bridge crossing the ESPOL lake (station 1+040), where potholes and slab joints from the underlying concrete are already reflected (Figure 14). Therefore, it is necessary to apply rehabilitation techniques that restore the structural capacity of the existing concrete slab, as proposed in this study. In specific cases where slabs are affected only by a few localized surface distresses with depths less than 4 cm, partial-depth repairs using epoxy concrete may be applied [35]. In the case of localized slab settlement, since the existing differential elevation indicates that the slab has cracked through its full depth, the proposed solution is likewise the full-depth replacement of part of the slab footprint or of the entire slab, including the reconditioning of the subbase layer.

For transverse and longitudinal cracks with shallow penetration (depths less than 7 cm), sealing with low-modulus silicone is recommended to prevent the ingress of water and the progression of the crack [42] For deeper longitudinal cracks (depths greater than 7 cm), the use of epoxy-resin sealant is proposed, as this material can fill the full-depth cavity of the crack and harden to a high compressive strength (≈75 MPa), allowing the structural capacity of the slab to be restored while preventing water infiltration [43]. These treatments must be accompanied by sealing the transverse and longitudinal joints with a hot-applied asphalt sealant, with an allowable deformation of 20–30%, and the installation of a polypropylene backer rod [44] to prevent water ingress and the recurrence of pumping-related deterioration. For longitudinal joints with irregular widths, where fluid sealants would be infeasible because the sealant would flow to the bottom of the joint, sealing with a preformed neoprene profile bonded with an epoxy adhesive between the slab and curb faces is recommended. Before joint sealing, deep cleaning and repair of spalled slab edges using high-strength epoxy concrete must be performed where necessary [38].

Table 18. Summary of rehabilitation procedures by damage group and severity

Group of Distress	Type of Distress	Severity	Rehabilitation Procedure
1. Surface distress	Potholes	Low	Partial-depth repair with epoxy concrete (if applicable)
		Medium	Partial-slab, full-depth replacement (depending on the affected area and the number of distresses)
		High	Full-depth total slab replacement
	Surface erosion	High	
	Spalling	Low	Partial-slab, full-depth replacement (depending on the affected area and the number of distresses)
		Medium	
		High	
2. Slab heave and settlement	Localized slab settlement	Low	
		Medium	
		High	
3. Joint sealant deficiency	Transverse joint sealant deficiency	Low	Joint sealing with hot-applied asphaltic seal
		Medium	
		High	
	Longitudinal joint sealant deficiency	Low	
		Medium	
		High	
4. Slab-to-curb separation			Joint sealing with a preformed neoprene seal
5. Cracking	Transverse crack	Low	Crack sealing with low-modulus silicone
		Medium	
		High	
	Longitudinal crack	Low	
		Medium	
		High	Crack sealing with epoxy resin
	Corner crack	Low	Crack sealing with low-modulus silicone
		Medium	
		High	Crack sealing with epoxy resin

The implementation of the proposed rehabilitation solutions will restore the structural condition and functionality of the concrete pavement slab. It is important to emphasize that the procedures must be carried out in accordance with the technical specifications of concrete pavement rehabilitation manuals, such as those outlined in the *Manual for the design and construction of concrete pavements* [31] or the *Concrete Pavement Preservation Guide* [38]. Otherwise, as highlighted by Smith et al. [38] and Van Dam et al. [39], the expected performance will not be achieved, and the rehabilitation investment will be compromised. Future rehabilitation activities must also be accompanied by periodic maintenance procedures executed with appropriate technical processes to prevent the onset of new distress caused by poorly executed practices [45, 46].

Table 18 presents a summary of the rehabilitation

techniques proposed for each distress group and severity level.

Additionally, Table 19 presents the rehabilitation cost analysis for 317 affected pavement slabs, totalling $198,735.15.

Table 19. Cost analysis of structural rehabilitation

Description	Unit	Quantity	Unit Price	Total Price
Partial (full-depth) / Total slab replacement				
Longitudinal cutting of rigid pavement	m	2011	$2.53	$5,087.83
Mechanical breaking of rigid pavement (Including debris removal)	m^3	457.11	$70.55	$32,249.1
Subbase layer (t = 15 cm)	m^3	10.32	$38.48	$397.11
Surface preparation with epoxy bonding agent	m^2	157.97	$16.78	$2,650.74
Ready-Mix concrete f'c = 300 kg/cm²	m^3	457.11	$175.29	$80,126.8
Joint sealing with asphaltic seal				
Joint cleaning	m	3392.5	$2.10	$7,124.25
Asphalt joint sealing	m	3392.5	$6.73	$22,831.5
Joint sealing with compression neoprene seal				
Joint cleaning	m	2000	$2.10	$4,200.00
Joint sealing with a preformed neoprene seal	m	2000	$20.56	$41,120.0
Crack sealing				
Crack cleaning (including edge cutting)	m	339.53	$2.04	$692.13
Crack sealing with low-modulus silicone	m	306.75	$4.91	$1,505.70
Crack sealing with epoxy resin	m	32.78	$22.92	$751.18
Total budget				$198,735.2

Therefore, the assessment of the slab condition through visual inspections and SD and ND testing enabled the development of a rehabilitation proposal based on targeted interventions that reduce material consumption and minimize the generation of construction and demolition waste by focusing on the most affected areas of the pavement slab, thereby providing more sustainable and efficient solutions. International experience shows that selective rehabilitation strategies can reduce life-cycle costs by 30–50% compared with full pavement reconstruction [42, 43]. Furthermore, recent studies on Chinese highways and comparative life-cycle cost analyses [47] corroborate that early preservation measures reduce cumulative maintenance and reconstruction costs.

Overall, the case study demonstrates that implementing a selective rehabilitation strategy is not only technically and economically feasible but also aligned with sustainability and emission-reduction objectives. The analysis developed in this study supports the technical and environmental validity of the proposed sustainable rehabilitation approach. Targeted interventions help reduce material consumption, minimize the generation of construction and demolition waste, and maintain the operational performance of the roadway infrastructure.

The methodology applied incorporates environmental and service-related criteria into the decision-making process, in accordance with the recommendations of the technical literature and the methodological guidelines defined in this article. The convergence between international technical practices and the evaluation process applied to the pavement slab, and the proposed rehabilitation strategy strengthens the potential for replicating this methodology in other university campuses with rigid RCCP pavements exposed to similar climatic and traffic conditions.

3.2.6 Comparative analysis and boundary conditions for the replicability of the methodology

This study is consistent with previous research showing that construction deficiencies, such as variations in slab thickness, poor compaction, and premature joint deterioration, are key determinants of the structural performance of RCCP pavements. Chhorn et al. [15] reported that irregularities in compaction and construction control directly influence the mechanical strength and durability of the pavement, even in projects executed under strict technical controls. Similarly, experimental studies on compaction methods have demonstrated a strong dependence between the construction process and the final strength of RCCP [17].

However, the replicability of the proposed methodology must be analyzed considering local boundary conditions. For example, research conducted in hot climates has shown that high ambient temperatures significantly affect the curing and strength gain of RCCP. Qasrawi et al. [47] evaluated compacted concrete mixtures under hot weather conditions, showing reductions in strength and changes in the microstructure of the material. Complementarily, Deghfel et al. [48] confirmed that temperatures above 40 °C and inadequate curing methods cause mechanical performance losses in RCCP pavements. These results are comparable to those of the case study, in which Guayaquil's tropical climate (high temperatures and humidity) likely accelerated the deterioration mechanisms observed.

In contrast, much of the international literature on the durability of RCCP comes from regions with cold climates, where mechanisms such as freeze-thaw damage and salt scaling predominate. For example, research in North America and Europe has analyzed the deterioration of RCCP under freezing conditions, reaching conclusions that are not directly transferable to tropical contexts [49]. This climatic difference shows that the results of this study should not be automatically extrapolated to other regions without methodological adjustments.

Traffic loads are another critical factor. International studies show that high percentages of heavy vehicles increase fatigue, rutting, and pumping on rigid pavements, accelerating their structural deterioration [17]. In this case, mixed traffic (light and heavy) accessing the ESPOL campus partly explains the concentration of damage in the final sections of the road, which coincides with performance reports on high-demand urban roads.

About concrete mix design, research has shown that variations in cement content, water-cement ratio, and aggregate type directly influence the strength and durability of RCCP. Studies with recycled materials (Reclaimed Asphalt Pavement (RAP) and rubber) show significant changes in the mechanical behavior of the pavement [50, 51], reinforcing the

need to calibrate the methodology according to local material properties.

Regarding life-cycle costs, the general literature suggests that selective rehabilitation strategies can reduce total costs by between 30% and 50% compared to complete reconstruction; however, this range depends heavily on the context (local prices, traffic, logistics, and the timing of the intervention). In the study, the damage survey shows that only a percentage of slabs require total replacement, while the majority are susceptible to partial repair and joint sealing.

However, to quantify these benefits more accurately, it is recommended to perform a Life Cycle Cost Analysis (LCCA) that incorporates discount rates, evaluation horizons, maintenance schedules, and user costs associated with traffic delays, following methodologies proposed for low-cost road management systems [52].

4. CONCLUSIONS

The structural condition of the 1,488-m RCCP section was evaluated through a comprehensive in-situ survey combined with SD and ND testing. Several construction errors and quality control deficiencies were identified, including slab dimensions that deviated from the standard design values (3.40 m width and 4.40 m length). Field measurements revealed widths ranging from 3.20 to 3.50 m and lengths between 4.10 and 4.85 m. Irregular slab thicknesses were also recorded, ranging from 19 to 26 cm. Internal voids were detected within the concrete, reducing compressive strength to as low as 8.14 MPa in the final roadway segments, far below the normative 30 MPa required for such traffic conditions. Abnormal longitudinal joint widths ranging from 1 to 3 cm compared to the 3 to 6 mm design range—were also documented, allowing water infiltration and promoting subsequent cracking through fines pumping, in addition to deficient joint seal maintenance and widespread longitudinal and transverse cracking. Overall, more than one-fifth (21.83%) of the slabs presented some distress.

The in-situ survey was complemented by a UAV-based assessment over the test segment, achieving a 95% detection rate relative to the ground survey with a flight altitude of no more than 10 m. However, the performance of this UAV must be interpreted with the limitations of the study in mind. The 95% detection rate was obtained on the 50 m pilot section selected for its high concentration of visible damage and favourable observation conditions; therefore, this result should be considered exploratory and not directly extrapolated to the 1.5 km of road. Furthermore, the recommendation for intervention should be understood within a prioritisation framework, in which maintenance and rehabilitation actions are guided by the severity and extent of the damage, the functional importance of the road, traffic demand, and budgetary constraints. In this context, the methodology supports a strategy of progressive and selective rehabilitation by identifying critical areas for intervention, while remaining replicable as long as it is adapted to local climate, traffic, and material conditions.

The evaluation revealed that the pavement's construction did not adhere to design specifications, and that adequate preparation or proper sequencing was not implemented during slab placement relative to the curb, resulting in insufficient compaction of the RCCP. Rehabilitation of the 317 affected slabs includes: (a) partial-slab (full-depth) or full-slab replacement at the designated locations; (b) hot-applied asphalt sealant for joint sealing; (c) preformed neoprene joint seal; and (d) sealing of cracks using low-modulus silicone sealant or epoxy resin. Future rehabilitation and maintenance work must be executed with proper quality control and trained technical personnel. Given the rate at which distresses are progressing, immediate rehabilitation of the pavement is recommended to prevent further deterioration.

This case study demonstrates that construction errors and inadequate quality control during the construction of an RCCP rigid pavement can significantly reduce its service life and performance level, resulting in accelerated deterioration, costly interventions, and risks to both project investment and roadway user safety. The integration of SD and ND tests within the structural evaluation methodology proved essential, as did the effectiveness of UAV flights for distress detection. The replicable methodology applied in this study facilitated the proposal of rehabilitation strategies aligned with SDGs 9 and 11.

Future evaluations could be strengthened by increasing the frequency of tests, extracting additional concrete cores to determine in-place strength, conducting supplementary ultrasonic and Ground-Penetrating Radar (GPR) surveys, and performing Life-Cycle Assessment (LCA) and LCCA to support the long-term sustainability of the proposed rehabilitation solutions.

ACKNOWLEDGMENTS

We extend our gratitude to the ESPOL research project "Registro de sitios de interés geológicos del Ecuador para estrategias de desarrollo sostenible" (Project Code CIPAT-004-2024). This study was conducted with the support of the Master's Program in Civil Engineering at ESPOL.

REFERENCES

[1] Stöckner, M., Buttgereit, A., Stöckner, U. (2025). Asset management of municipal road infrastructure. In Advances in Information Technology in Civil and Building Engineering, pp. 228-240. https://doi.org/10.1007/978-3-031-84224-5_18

[2] Smith, R.L. (2008). Premodern Trade in World History. Routledge. https://doi.org/10.4324/9780203893524

[3] World Bank. (2024). Infrastructure development thrives under robust public-private partnership regulatory frameworks, World Bank report shows. https://www.bancomundial.org/es/topic/sustainableinfrastructurefinance/brief/infrastructure-development-thrives-under-robust-ppp-regulatory-frameworks-world-bank-report-shows.

[4] Mitchell, M.F., Walker, R.N. (1985). The economics of pavement type selection. In the 3rd International Conference on Concrete Pavement Design and Rehabilitation, Purdue University, West Lafayette, Indiana, USA, pp. 23-32. https://doi.org/10.33593/iccp.v3i1.1078

[5] De Solminihac, H., Bustos, M.G., Altamira, A.L., Covarrubias, J.P. (2003). Functional distress modelling in Portland cement concrete pavements. Canadian Journal of Civil Engineering, 30(4): 696-703. https://doi.org/10.1139/l03-016

[6] Rui, H.T., Wu, Q.Q., Zhao, Y.F., Zhang, S.Z. (2012). Influence of highway construction on regional economy development—Taking Shaanxi as an example. Journal of Chang'an University (Natural Science Edition), 32(6): 83-87. https://www.scopus.com/pages/publications/84872161687.

[7] Velasco, C., Eguez, H. (2009). Mechanical properties of a paver-compacted concrete design with fast track working together. Escuela Superior Politécnica del Litoral. https://www.dspace.espol.edu.ec/handle/123456789/142.

[8] LaHucik, J., Roesler, J. (2017). Field and laboratory properties of roller-compacted concrete pavements. Transportation Research Record: Journal of the Transportation Research Board, 2630: 33-40. https://doi.org/10.3141/2630-05

[9] Batouli, M., Bienvenu, M., Mostafavi, A. (2017). Putting sustainability theory into roadway design practice: Implementation of LCA and LCCA analysis for pavement type selection in real world decision making. Transportation Research Part D: Transport and Environment, 52: 289-302. https://doi.org/10.1016/j.trd.2017.02.018

[10] Zambrano, T., Basantes, C. (2013). Analysis and proposed solutions for deformations in paver-compacted concrete (HCP) slabs of rigid pavement: A case study of the main road of the Gustavo Galindo Velasco campus at Escuela Superior Politécnica del Litoral. Escuela Superior Politécnica del Litoral, Guayaquil, Ecuador. http://www.dspace.espol.edu.ec/xmlui/handle/123456789/32517.

[11] Hegger, J., Bertram, G. (2008). Shear carrying capacity of Ultra-High Performance Concrete beams. In Tailor Made Concrete Structures: New Solutions for Our Society, pp. 341-347. http://www.abece.com.br/web/restrito/restrito/pdf/ch049.pdf.

[12] Subedi, A., Jeong, K.D., Lee, M.S., Lee, S.J. (2025). Effectiveness of diamond grinding in enhancing rigid pavement performance: A review of key metrics. Applied Sciences, 15(16): 8980. https://doi.org/10.3390/app15168980

[13] Briones-Bitar, J., Pinto-Ponce, B., Caicedo-Potosí, J., Santos-Baquerizo, E., Carrión-Mero, P., Morante-Carballo, F. (2025). Evolution of smart buildings: A bibliometric analysis and systematic review. International Journal of Sustainable Development and Planning, 20(4): 1369-1383. https://doi.org/10.18280/ijsdp.200403

[14] Fay, M., Andrés, L.A., Fox, C., Narloch, U., Straub, S., Slawson, M. (2017). Rethinking infrastructure in Latin America and the Caribbean: Spending better to achieve more. World Bank. https://documents1.worldbank.org/curated/en/671711491563967405/pdf/114110-REVISED-Rethinking-Infrastructure-Low-Res.pdf.

[15] Chhorn, C., Hong, S.J., Lee, S.W. (2017). A study on performance of roller-compacted concrete for pavement. Construction and Building Materials, 153: 535-543. https://doi.org/10.1016/j.conbuildmat.2017.07.135

[16] Aghaipour, A., Madhkhan, M. (2020). Mechanical properties and durability of roller compacted concrete pavement (RCCP) – A review. Road Materials and Pavement Design, 19(8): 1775-1798. https://doi.org/10.1080/14680629.2019.1579754

[17] Krishna, S., Sravana, P., Chandrasekhara, T. (2016). Experimental studies in ultrasonic pulse velocity of roller compacted concrete pavement containing fly ash and M-sand. International Journal of Pavement Research and Technology, 9(4): 345-352. https://doi.org/10.1016/j.ijprt.2016.08.003

[18] Morante, F., Santos, E., Pinto, B., Chacón, E., Briones, J., Carrión, P. (2024). Proposal for the rehabilitation of household in seismic vulnerability zones. International Journal of Safety and Security Engineering, 14(3): 701-716. https://doi.org/10.18280/ijsse.140304

[19] National Institute of Roads. (2006). Manual for the visual inspection of rigid pavements. Ministry of Transport of Colombia. https://es.slideshare.net/slideshow/manual-para-inspeccion-de-pavimentos-rigidos-pdf/271662628.

[20] Aliha, M.R.M., Karimi, H.R., Khedri, E., Abdipour, S.V., Haghighatpour, P.J. (2024). Rehabilitation and reinforcement of cracked pavements using crack sealers and composite patches. Heliyon, 10(19): e38145. https://doi.org/10.1016/J.HELIYON.2024.E38145

[21] Feitosa, I., Santos, B., Almeida, P.G. (2024). Pavement inspection in transport infrastructures using unmanned aerial vehicles (UAVs). Sustainability, 16(5): 2207. https://doi.org/10.3390/su16052207

[22] American Concrete Institute. (2014). ACI 546R-14: Concrete repair guide. American Concrete Institute. https://www.concrete.org/Portals/0/Files/PDF/Previews/546R_14_PREVIEW.pdf.

[23] ASTM International. (2020). ASTM C42/C42M-20: Standard test method for obtaining and testing drilled cores and sawed beams of concrete. ASTM International. https://doi.org/10.1520/C0042_C0042M-20

[24] ASTM International. (2016). ASTM C597-16: Standard test method for pulse velocity through concrete. ASTM International. https://doi.org/10.1520/C0597-16

[25] ASTM International. (2018). ASTM C805/C805M-18: Standard test method for rebound number of hardened concrete. ASTM International. https://doi.org/10.1520/C0805_C0805M-18

[26] Asociación Española de Normalización y Certificación. (2007). UNE-EN 14630:2007. Products and systems for the protection and repair.

[27] Taman, M., Abd Elaty, M., Behiry, R.N. (2022). Codes applicability of estimating the FRC compressive strength by the core-drilling method. Construction and Building Materials, 330: 127227. https://doi.org/10.1016/J.CONBUILDMAT.2022.127227

[28] Kamekura Seiki Co., Ltd. (2015). Concrete Test Hammer R-7500: Operating manual. Kamekura Seiki Co., Ltd. https://www.eg.aktio.co.jp/wp-content/uploads/R3K21070002_R-7500_torisetu.pdf.

[29] Goueygou, M., Abraham, O., Lataste, J.F. (2008). A comparative study of two non-destructive testing methods to assess near-surface mechanical damage in concrete structures. NDT & E International, 41(6): 448-456. https://doi.org/10.1016/J.NDTEINT.2008.03.001

[30] British Standards Institution. (2021). BBS EN 12504-4:2021. Testing concrete in structures - Determination of ultrasonic pulse velocity. https://knowledge.bsigroup.com/products/testing-

concrete-in-structures-determination-of-ultrasonic-pulse-velocity.
[31] Calo, D., Souza, E., Marcolini, E. (2014). Manual for the design and construction of concrete pavements. Argentine Portland Cement Institute. https://icpa.org.ar/descarga-manual-de-diseno-y-construccion-de-pavimentos-de-hormigon/.
[32] Harrington, D., Ayers, M., Cackler, T., Fick, G., et al. (2018). Guide for concrete pavement distress assessments and solutions: Identification, causes, prevention, and repair. National Concrete Pavement Technology Center, Iowa State University. https://www.intrans.iastate.edu/wp-content/uploads/2019/01/concrete_pvmt_distress_assessments_and_solutions_guide_w_cvr.pdf.
[33] Calo, D., Polzinetti, M. (2016). Manual of urban concrete pavements. Argentine Portland Cement Institute. https://icpa.org.ar/wp-content/uploads/2019/04/Manual_Pavimentos_Urbanos_de_Hormigon.pdf.
[34] Lv, Z., Hao, Z., Zhu, Y., Lu, C. (2025). A review on automated detection and identification algorithms for highway pavement distress. Applied Sciences, 15(11): 6112. https://doi.org/10.3390/app15116112
[35] Inzerillo, L., Acuto, F., Di Mino, G., Uddin, M.Z. (2022). Super-resolution images methodology applied to UAV datasets to road pavement monitoring. Drones, 6(7): 171. https://doi.org/10.3390/drones6070171
[36] Alwash, M., Breysse, D., Sbartaï, Z.M., Szilágyi, K., Borosnyói, A. (2017). Factors affecting the reliability of assessing the concrete strength by rebound hammer and cores. Construction and Building Materials, 140: 354-363. https://doi.org/10.1016/J.CONBUILDMAT.2017.02.129
[37] Selvam, M., Singh, S. (2023). Review on influence of compaction mechanisms on roller compacted concrete pavement performance. ACI Materials Journal, 120(1): 155-168. https://doi.org/10.14359/51737290
[38] Smith, K., Grogg, M., Ram, P., Smith, K., Harrington, D. (2022). Concrete Pavement Preservation Guide (3rd ed.). Concrete Pavement Technology Center, Iowa State University. https://www.intrans.iastate.edu/wp-content/uploads/2022/08/concrete_pvmt_preservation_guide_3rd_edition_web.pdf.
[39] Van Dam, T.J., Smith, K.D., Harrington, D., Pierce, L., Ram, P. (2019). Strategies for concrete pavement preservation (FHWA-HIF-18-025). Federal Highway Administration. https://www.fhwa.dot.gov/pavement/pubs/hif18025.pdf.
[40] Treviño, M., Dossey, T., McCullough, B.F., Yildirim, Y. (2003). Applicability of asphalt concrete overlays on continuously reinforced concrete pavements. Center for Transportation Research, The University of Texas Austin. https://library.ctr.utexas.edu/ctr-publications/0-4398-1.pdf.
[41] Riekstins, A., Haritonovs, V., Straupe, V. (2020). Life cycle cost analysis and life cycle assessment for road pavement materials and reconstruction technologies. The Baltic Journal of Road and Bridge Engineering, 15(5): 118-135. https://doi.org/10.7250/bjrbe.2020-15.510
[42] Torres-Machí, C., Evers, E., Schmidt, J., Crayton, A. (2024). Pavement rehabilitation analysis: A life-cycle cost and long-term performance comparison of full depth reclamation and overlays (Report No. CDOT-2024-07). Colorado Department of Transportation. https://rosap.ntl.bts.gov/view/dot/75734/dot_75734_DS1.pdf.
[43] Lu, L., Zhao, D., Fan, J., Li, G. (2021). A brief review of sealants for cement concrete pavement joints and cracks. Road Materials and Pavement Design, 23(7): 1467-1491. https://doi.org/10.1080/14680629.2021.1898452
[44] U.S. Department of Defense. (2018). UFC 3-270-01: O&M manual – Asphalt and concrete pavement maintenance and repair (Change 1, 2022). Unified Facilities Criteria. https://www.wbdg.org/FFC/DOD/UFC/ufc_3_270_01_2018_c1.pdf.
[45] Torres-Machí, C., Evers, E., Schmidt, J., Crayton, A. (2024). Pavement rehabilitation analysis: A life-cycle cost and long-term performance comparison of full depth reclamation and overlays (Report No. CDOT-2024-07). Colorado Department of Transportation. https://rosap.ntl.bts.gov/view/dot/75734/dot_75734_DS1.pdf.
[46] Guven, Z. (2006). Life Cycle Cost Analysis of Pavements: State of the Practice. Master dissertation, Clemson University. https://open.clemson.edu/all_theses/57.
[47] Qasrawi, H.Y., Asi, I.M., Wahhab, H.I.A.A. (2005). Proportioning RCCP mixes under hot weather conditions for a specified tensile strength. Cement and Concrete Research, 35(2): 267-276. https://doi.org/10.1016/j.cemconres.2004.04.030
[48] Deghfel, M., Meddah, A., Beddar M., Chikouche, M.A. (2019). Experimental study on the effect of hot climate on the performance of roller-compacted concrete pavement. Innovative Infrastructure Solutions, 4: 54. https://doi.org/10.1007/s41062-019-0246-8
[49] Ramezanianpour, A.A., Mohammadi, A., Dehkordi, E.R., Chenar, Q. (2017). Mechanical properties and durability of roller compacted concrete pavements in cold regions. Construction and Building Materials, 146: 260-266. https://doi.org/10.1016/j.conbuildmat.2017.04.099
[50] Meddah, A., Beddar, M., Abderrahim, B. (2014). Use of shredded rubber tire aggregates for roller compacted concrete pavement. Journal of Cleaner Production, 72: 187-192. https://doi.org/10.1016/j.jclepro.2014.02.052
[51] Settari, C., Debieb, F., Kadri, E.H., Boukendakdji, O. (2015). Assessing the effects of recycled asphalt pavement materials on the performance of roller compacted concrete. Construction and Building Materials, 101: 617-621. https://doi.org/10.1016/j.conbuildmat.2015.10.039
[52] Khahro, S.H., Memon, Z.A., Gungat, L., Yazid, M.R.M., et al. (2021). Low-cost pavement management system for developing countries. Sustainability, 13(11): 5941. https://doi.org/10.3390/su13115941

NOMENCLATURE

R	dimensionless rebound number
Rc	dimensionless corrected rebound number
ΔR	dimensionless direction correction factor for rebound number

ΔRw	dimensionless moisture correction factor for rebound number
f'c	compressive strength of concrete, MPa = 1 kg/(1000s*m)
t	time, s
X	distance, m
h	crack depth
d	distress depth, cm
w	distress width, cm
dif	vertical differential, cm
l	% affected of joint length, %
cw	crack width, mm

Greek symbols

α_n	dimensionless age factor for rebound number

Subscripts

RCCP	Roller-Compacted Concrete Pavement